

Non-polar GaN quantum dots integrated into high quality cubic AlN microdisks

M. Bürger^{*1}, G. Callsen², T. Kure², A. Hoffmann², A. Pawlis¹, D. Reuter¹, and D. J. As¹

¹ Universität Paderborn, Department Physik, Warburger Str. 100, 33098 Paderborn, Germany

² Institut für Festkörperphysik, Technische Universität Berlin, Hardenbergstr. 36, 10623 Berlin, Germany

Received 14 August 2013, revised 8 October 2013, accepted 28 November 2013

Published online 22 January 2014

Keywords GaN, microdisk, quantum dots, molecular beam epitaxy

* Corresponding author: e-mail mbuerger@mail.uni-paderborn.de, Phone: +49 5251 60 5848, Fax: +49 5251 60 5831

We report on lasing of non-polar GaN quantum dots which are integrated into novel cubic AlN microdisks. Optical spectroscopy of freestanding microdisks at low temperature (~10 K) revealed distinct whispering gallery modes with quality factors up to $Q \sim 3000$ in the high energy range around ~4 eV of microdisks with a diameter of 4 μm . Furthermore, we obtained S-shaped curves of

the integral mode intensity, accompanied by a significant linewidth narrowing in power dependent micro-photoluminescence experiments. The spontaneous emission coupling factors were determined to $\beta = 0.26$ and $\beta = 0.58$ with respect to the radial order of the resonator modes.

© 2014 WILEY-VCH Verlag GmbH & Co. KGaA, Weinheim

1 Introduction Optical microresonators based on group III-nitrides have attracted large interest for light sources in the ultraviolet spectral range. Microdisks are of particular relevance as they offer low loss and high confined whispering gallery modes (WGMs) due to internal total reflection at the disk boundary [1]. For this propose promising applications are provided by microdisks in quantum information technology like single photon sources or low threshold cavity lasers [2,3]. Especially, microdisks containing quantum dots (QDs) as active material are suitable for low threshold-power and highly gained lasers. Enhanced spontaneous emission of QDs coupling to WGMs (Purcell Effect [4]), up to the point of laser emission, has already been observed in several semiconductor materials [5,6]. Group III-nitrides microdisks containing QDs are a promising candidate for ultraviolet light sources.

In wurtzite GaN QDs the Quantum Confined Stark Effect caused by internal piezoelectric and spontaneous polarization fields along the polar c-axis leads to spatially separated electron and holes in confined states. These built-in electric fields are causally related to radiative lifetimes ranging from 100 ps up to several μs , which is the main obstacle to achieve lasing in such microdisks [7]. To avoid internal fields group III-nitrides can be grown in the

metastable cubic phase along the (001) direction on 3C-SiC substrates [8,9]. Due to the absence of electric fields, a two orders of magnitude lower recombination time of non-polar cubic GaN (c-GaN) QDs compared to hexagonal (h-GaN) QDs was observed [10,11]. Lasing emission of microdisks containing bulk h-GaN and h-InGaN quantum wells (QWs) as active material has already been demonstrated [12,13].

In this paper we analyze the laser emission of non-polar c-GaN QDs embedded in c-AlN microdisks under pulsed optical excitation. Freestanding microdisks were fabricated and optically characterized by power dependent micro-photoluminescence ($\mu\text{-PL}$) measurements at ~10 K. Our experiments show an alternative approach to realize ultraviolet light sources besides the already reported h-GaN QD based microcavities (microdisks, Q-factor ~ 7000 [14] and photonic crystal cavities, Q-factor ~ 5000 [15]).

2 Experimental The samples were grown on 10 μm (001) 3C-SiC substrates on top of 500 μm Si by plasma assisted molecular beam epitaxy. Initially a 30 nm c-AlN barrier layer was deposited followed by a single c-GaN QDs layer at 760 °C substrate temperature. The Stranski

Krastanov growth mode was used to form self assembled QDs. To cover the active QD layer, another 30 nm c-AlN barrier layer was grown on top. Typical QDs densities of similar uncapped samples are in the order of 10^{11} cm^{-2} as determined by scanning atomic force microscopy (AFM) measurements [16]. A detailed growth procedure of c-AlN and c-GaN QDs was previously described in our earlier work [17]. The microdisks were patterned by electron beam lithography followed by two consecutive dry chemical etching steps [18].

We characterized the microdisks optically in a confocal μ -PL setup. The fourth harmonic of a Nd:YAG laser (Coherent Antares 76s) at 266 nm (4.66 eV) with a pulse length of 60 ps was used for optical excitation. The laser beam was therefore focused by a microscope objective (NA = 0.4) to a $\sim 1 \mu\text{m}$ diameter laser spot at the edge of the microdisk. A subtractive 1 m monochromator (Spex 1704) with a spectral resolution of $\sim 300 \mu\text{eV}$ was used for spectral separation. Due to the pumping energy of 4.66 eV carrier excitation in the c-AlN barriers (direct bandgap 5.93 eV, indirect bandgap 5.3 eV) [19]) is negligible. Consequently, the main absorption can be expected to take place in the single QD layer. Using dielectric constants of $\epsilon_1 = 7$ and $\epsilon_2 = 1.8$ we calculated the absorption coefficient to $\alpha_{\text{c-GaN}}(4 \text{ eV}) = 0.012 \text{ nm}^{-1}$ [20]. Taking into account a height z for the QDs, the absorption can be derived by $I(z) = I_0 \exp(-\alpha_{\text{c-GaN}} z)$. Assuming a homogenous spatial distribution and a height of $z \cong 3 \text{ nm}$ for the QDs, obtained from AFM measurements [16] the absorbed power in the active layer can be estimated to be only $\sim 4 \%$. Additional loss due to reflection at the sample surface can be calculated for perpendicular incidence to $\sim 13 \%$ using $n_{\text{air}} = 1$ and $n_{\text{c-AlN}} = 2.1$ at 4 eV [19,21]. All excitation powers mentioned in this work were corrected values in the manner described above.

3 Results and discussion In Fig. 1(a) a PL spectrum of a $4 \mu\text{m}$ diameter microdisk at $\sim 10 \text{ K}$ is depicted. The c-GaN QDs luminescence forms a Gaussian shaped emission band around 3.62 eV, with a FWHM of 228 meV [22]. QD emission resonant with WGMs is enhanced by the Purcell factor and superimposes the PL spectrum by several narrow peaks mainly on the high energy side. The inset of Fig. 1 (a) shows a side view scanning electron microscopy image of a freestanding $4 \mu\text{m}$ microdisk on a 3C-SiC substrate post. There are some possible reasons for the small number of WGMs: On the one hand scattering of resonant modes at vertical striations at the disk sidewall can inhibit the appearance of WGMs [23]. On the other hand a perfect microdisk has an in plane emission characteristic and we collect therefore only a small fraction of the emission, which is scattered out at these imperfections. Furthermore the relative broad post underneath the freestanding slab probably leads to absorption of circulating waves.

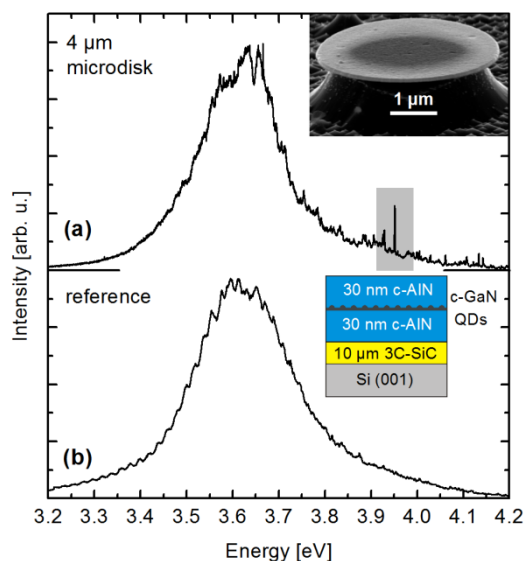


Figure 1 PL spectra in the range from 3.2 eV to 4.2 eV taken at $\sim 10 \text{ K}$ of a (a) $4 \mu\text{m}$ microdisk and (b) of an unprocessed part of the sample as reference. Insets: (a) Side view scanning electron microscopy image of a $4 \mu\text{m}$ microdisk and (b) a schematic layer structure of the unstructured sample. The high energy range of the microdisk with striking WGMs is grey colored (a).

The PL spectrum of an unprocessed part of our sample is shown in Fig. 1(b) for reference. An emission band of the QD ensemble peaking at 3.63 eV with a similar FWHM of 212 meV dominates the PL spectrum. Fabry-Pérot layer oscillations of the $10 \mu\text{m}$ 3C-SiC substrate superimpose the reference spectrum on the low energy side, but sharp WGMs cannot be identified. Due to the QD density of 10^{11} cm^{-2} both ensemble emission bands in Fig 1 can be correlated to the size distribution of the QDs [24].

In the following we evaluate the lasing characteristics of particular WGMs. To achieve lasing, the excitation power has to be increased until the threshold is reached and stimulated emission occurs. In our PL measurements we vary the optical excitation power from 3 kWcm^{-2} to 631 kWcm^{-2} . Figure 2 displays PL spectra of a $4 \mu\text{m}$ microdisk on the high energy side (grey colored rectangle in Fig. 1 (a)) in the range from 3.92 eV to 3.98 eV for 5 different excitation powers. The two highlighted lasing modes at 3.930 eV (A) and at 3.952 eV (B) were analyzed in detail. Weak intensities of the WGMs at low excitation powers indicate a linear increase of the mode intensity up to $\sim 30 \text{ kWcm}^{-2}$. A further increase of the excitation power up to 631 kWcm^{-2} leads to dominant WGMs pointing to laser operation.

The QD ensemble spectrum shows weak intensities on the low and high energy side indicating a low QD density emitting at these energies. We attribute the relatively low intensities of the WGMs compared to that of the QD ensemble to the small number of QDs which are emitting into a lasing mode [25]. In our case the high energy modes are

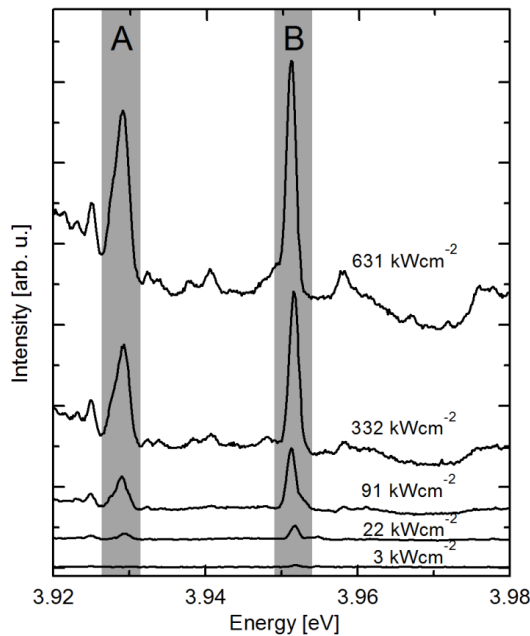


Figure 2 Power dependence of the PL spectra in the high energy region. The excitation power was increased from 3 kWcm⁻² to 631 kWcm⁻² as denoted for each spectrum. The analyzed lasing modes A at 3.930 eV and B at 3.952 eV are highlighted in grey.

of particular interest for a microcavity laser based on single QDs.

Figure 3 depicts the input-output characteristic of mode A at 3.930 eV and mode B at 3.952 eV. The integrated mode intensities obtained from mode A and B are plotted by filled circles in a double logarithmic scale as a function of the excitation power. Dashed lines indicate the offset between the spontaneous emission and the lasing regime by low and high power asymptotes. The β -factor describes the fraction of the spontaneous emission that couples into the lasing mode. Conventional lasers with $\beta \ll 1$ show a kink at the transition from low to high power followed by a superlinear increase of the output intensity. Semiconductor microcavity lasers with a small mode volume can reach β -factors close to 1 [6,26,27] resulting in a smeared kink at threshold. We observe clearly S-shaped threshold behaviors and smooth transitions from spontaneous to stimulated emission for both modes in Fig. 3. The typical kink appears for mode A at a threshold of ~ 30 kWcm⁻² and for mode B at ~ 10 kWcm⁻². The small offset between lasing and nonlasing suggests high β values and results in efficient coupling between the QDs and the cavity modes. We determined β -factors of 0.26 and 0.58 for mode A and B, respectively. WGMs of higher radial orders lead to a weaker coupling between the QD emission and the resonator modes, which usually results in smaller β -factors (cf. mode A).

To verify the QD lasing in our microdisks we compare the experimental results with a theoretical model for semiconductor microcavity lasers described in Ref. [27]. This

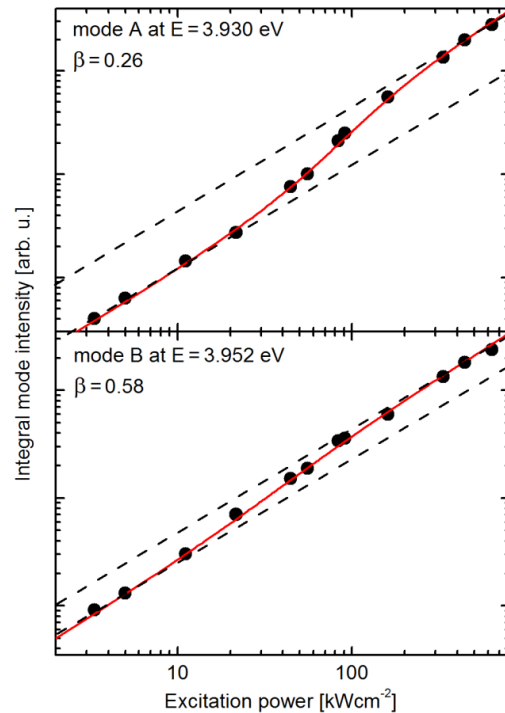


Figure 3 Input-output characteristic of lasing mode A at 3.930 eV and mode B at 3.952 eV (integral mode intensity as a function of the excitation power). The experimental results are indicated by filled circles, the solid lines display fits according Eq. (1). The dashed lines show the asymptotes to low and high power operation.

analytical derivation based on rate equations expresses the excitation intensity I as a function of the photon number p for negligible nonradiative losses by

$$I(p) = \frac{q\gamma}{\beta} \left[\frac{p}{1+p} (1+\xi)(1+\beta p) - \xi\beta p \right]. \quad (1)$$

Here γ denotes the cavity decay rate, q the electron charge and ξ the mean number of emitted photons in the cavity. The best fit results for the experimental data were obtained using γ -factors of 19 ($\xi = 0.3$) and 23 ($\xi = 0.1$) for mode A and B, respectively. Solid lines in Fig. 3 illustrate the fits according to the theoretical model.

Figure 4 shows the modification of the linewidth of lasing mode A with increasing excitation power. The accuracy was estimated to be ± 0.3 meV. A typical narrowing until the lasing threshold is reached followed by an increase of the linewidth can be observed [6,26]. The minimum achievable linewidth of a laser is known as the Schawlow Townes linewidth [28]. We find at ~ 30 kWcm⁻² a minimum FWHM of 1.3 meV resulting in a Q-factor of ~ 3000 . Around the laser threshold, absorption losses of the resonator are compensated by stimulated emission and optical transparency is reached. After crossing the threshold the linewidth increases up to 3.2 meV. We attribute this increase of the linewidth to free carrier absorption at high excitation powers [29].

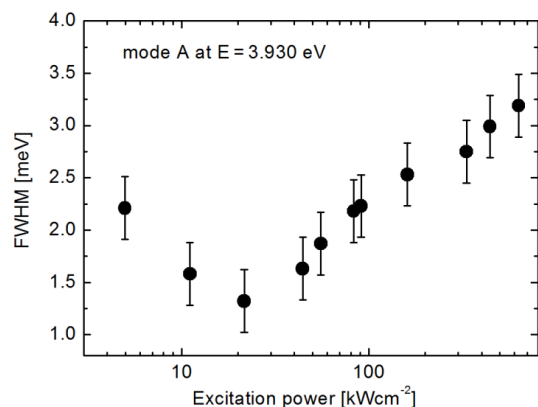


Figure 4 Linewidth of mode A at 3.930 eV as a function of the optical pump power.

4 Conclusions We demonstrate lasing emission of non-polar GaN QDs embedded in cubic AlN microdisks. One layer of self-assembled Stranski-Krastanov QDs enclosed in 30 nm cubic AlN barriers was grown by molecular beam epitaxy. A 4 μm diameter microdisk was investigated by power dependent $\mu\text{-PL}$ studies at low temperatures in view of lasing emission. Typical S-shaped input-output characteristics for small volume semiconductor microcavity lasers as well as a significant reduction of the emission linewidth revealed lasing emission of our microdisks. The nonlinear increase of the emission intensity started at a threshold of $\sim 10 \text{ kWcm}^{-2}$ accompanied with cavity modes reaching Q-factors up to ~ 3000 . The spontaneous emission coupling (β -factors) into a lasing mode were estimated to $\beta = 0.26$ and $\beta = 0.58$. Our results move the upper bound for microdisk QD lasing to the ultraviolet spectral range and offer strong potential of low-threshold power microcavity lasers based on cubic AlN/GaN QDs.

Acknowledgements This work was supported by the DFG graduate program GRK 1464 “Micro- and Nanostructures in Optoelectronics and Photonics” and the Collaborative Research Center (SFB 787). Furthermore this research was supported by the Commissioned Research of the National Institute of Information and Communications Technology (NICT), the Ministry of Education, Culture, Sports, Science and Technology (MEXT), and the Funding Program for World-leading Innovative Research and Development on Science and Technology (FIRST).

References

- [1] S.L. McCall, A.F.J. Levi, R.E. Slusher, S.J. Pearton, and R.A. Logan, *Appl. Phys. Lett.* **60**, 289 (1992).
- [2] A. Pawlis, M. Panfilova, D.J. As, K. Lischka, K. Sanaka, T.D. Ladd, Y. Yamamoto, *Phys. Rev. B* **77**, 153304 (2008).
- [3] K. J. Vahala, *Nature* **424**, 839 (2003).
- [4] J. M. Gérard and B. Gayral, *J. Lightwave Technol.* **17**, 2089 (1999).
- [5] E. Peter, I. Sagnes, G. Guirleo, S. Varoutsis, J. Bloch, A. Lemaître, and P. Senellart, *Appl. Phys. Lett.* **86**, 021103 (2005).
- [6] J. Renner, L. Worschech, A. Forchel, S. Mahapatra, and K. Brunner, *Appl. Phys. Lett.* **89**, 231104 (2006).
- [7] S. Kako, M. Miyamura, K. Tachibana, K. Hoshino, and Y. Arakawa, *Appl. Phys. Lett.* **83**, 984 (2003).
- [8] D.J. As, *Microelectron. J.* **40**, 204 (2009).
- [9] B. Daudin, G. Feuillet, J. Hübner, Y. Samson, F. Widmann, A. Philippe, C. Bru-Chevallier, G. Guillot, E. Bustarret, G. Bentoumi, and A. Deneuveville, *J. Appl. Phys.* **84**, 2295 (1998).
- [10] J. Simon, N. T. Pelekanos, C. Adelman, E. Martinez-Guerrero, R. André, B. Daudin, Le Si Dang, and H. Mariette, *Phys. Rev. B* **68**, 035312 (2003).
- [11] T. Bretagnon, P. Lefebvre, P. Valvin, R. Bardoux, T. Guillet, T. Taliercio, and B. Gil, *Phys. Rev. B* **73**, 113304 (2006).
- [12] A. C. Tamboli, E. D. Haberer, R. Sharma, K. H. Lee, S. Nakamura, and E. L. Hu, *Nature Photon.* **1**, 61 (2007).
- [13] H. W. Choi, K. N. Hui, P. T. Lai, P. Chen, X. H. Zhang, S. Tripathy, J. H. Teng, and S. J. Chua, *Appl. Phys. Lett.* **89**, 211101 (2006).
- [14] M. Mexis, S. Sergent, T. Guillet, C. Brimont, T. Bretagnon, B. Gil, F. Sémoud, M. Leroux, D. Néel, S. David, X. Chéourry, and P. Boucaud, *Opt. Lett.* **36**, 2203 (2011).
- [15] S. Sergent, M. Arita, S. Kako, S. Iwamoto, and Y. Arakawa, *Appl. Phys. Lett.* **100**, 121103 (2012).
- [16] M. Bürger, T. Schupp, K. Lischka, and D.J. As, *Phys. Status Solidi C* **9**, 1273 (2012).
- [17] T. Schupp, T. Meisch, B. Neuschl, M. Feneberg, K. Thonke, K. Lischka, and D.J. As, *AIP Conf. Proc.* **1292**, 165 (2010).
- [18] M. Bürger, M. Ruth, S. Declair, J. Förstner, C. Meier, and D.J. As, *Appl. Phys. Lett.* **102**, 081105 (2013).
- [19] M. Röppischer, R. Goldhahn, G. Rossbach, P. Schley, C. Cobet, N. Esser, T. Schupp, K. Lischka, and D. J. As, *J. Appl. Phys.* **106**, 076104 (2009).
- [20] M. Feneberg, M. Röppischer, C. Cobet, N. Esser, J. Schörmann, T. Schupp, D.J. As, F. Hörich, J. Bläsing, A. Krost, and R. Goldhahn, *Phys. Rev. B* **85**, 155207 (2012).
- [21] R. E. Slusher, A. F. J. Levi, U. Mohideen, S. L. McCall, S. J. Pearton, and R. A. Logan, *Appl. Phys. Lett.* **63**, 1310 (1993).
- [22] T. Schupp, K. Lischka, and D.J. As, *J. Cryst. Growth* **323**, 286 (2011).
- [23] S. Sergent, J. C. Moreno, E. Frayssinet, Y. Laaroussi, S. Chenot, J. Renard, D. Sam-Giao, B. Gayral, D. Néel, and S. David, *J. Phys.: Conf. Ser.* **210**, 012005 (2010).
- [24] G. Schmid, *Nanoparticles: From Theory to Application*, (Wiley-VCH, New York, 2006), p. 28.
- [25] M. Bürger, G. Callsen, T. Kure, A. Hoffmann, A. Pawlis, D. Reuter and D.J. As, *Appl. Phys. Lett.* **103**, 021107 (2013).
- [26] M. Witzany, R. Roßbach, W.-M. Schulz, M. Jetter, P. Michler, T.-L. Liu, E. Hu, J. Wiersig, and F. Jahnke, *Phys. Rev. B* **83**, 205305 (2011).
- [27] G. Björk and Y. Yamamoto, *IEEE J. Quantum Electron.* **27**, 2386 (1991).
- [28] A. L. Schawlow and C. H. Townes, *Phys. Rev.* **112**, 1940 (1958).
- [29] D. K. Young, L. Zhang, D. D. Awschalom, and E. L. Hu, *Phys. Rev. B* **66**, 081307 (2002).